Challenge Journal of Structural Mechanics

Research Article

Eigenvector and eigenvalue analysis of thick plates resting on elastic foundation with first order finite element

Yaprak I. Özdemir *

Department of Civil Engineering, Karadeniz Technical University, 61080 Trabzon, Turkey

ABSTRACT

The purpose of this paper is to study free vibration analysis of thick plates resting on Winkler foundation using Mindlin's theory with first order finite element, to determine the effects of the thickness/span ratio, the aspect ratio, subgrade reaction modulus and the boundary conditions on the frequency parameters of thick plates subjected to free vibration. In the analysis, finite element method is used for spatial integration. Finite element formulation of the equations of the thick plate theory is derived by using first order displacement shape functions. A computer program using finite element method is coded in C++ to analyze the plates free, clamped or simply supported along all four edges. In the analysis, 4-noded finite element is used. Graphs are presented that should help engineers in the design of thick plates subjected to earthquake excitations. It is concluded that 4-noded finite element can be effectively used in the free vibration analysis of thick plates. It is also concluded that, in general, the changes in the thickness/span ratio are more effective on the maximum responses considered in this study than the changes in the aspect ratio.

ARTICLE INFO

Article history:
Received 21 February 2018
Revised 30 March 2018
Accepted 19 April 2018

Keywords:
Parametric free vibration analysis
Thick plate
Mindlin's theory
First order finite element
Winkler foundation

1. Introduction

Plates are structural elements which are commonly used in the building industry. A plate is considered to be a thin plate if the ratio of the plate thickness to the smaller span length is less than 1/20; it is considered to be a thick plate if this ratio is larger than 1/20 (Ugural, 1981).

The dynamic behavior of thin plates has been investigated by many researchers (Warburton, 1954; Leissa, 1973, 1977a, 1977b, 1981a, 1981b, 1987a, 1987b; Caldersmith, 1984; Sakata and Hosokawa, 1988; Providakis and Beskos, 1989a, 1989b; Ayvaz and Durmuş, 1995; Lok and Cheng, 2001; Grice and Pinnington, 2002; Si et al., 2005). There are also many references on the behavior of the thick plates subjected to different loads. The studies made on the behavior of the thick plates are based on the Reissner-Mindlin plate theory (Reissner, 1945, 1947, 1950; Mindlin, 1951). This theory requires only C^0 continuity for the finite elements in the analysis of thin and thick plates. Therefore, it appears as an alternative to the thin plate theory which also requires C^1 continuity. This requirement in the thin plate theory is solved easily if Mindlin's theory is used in the analysis of thin plates. Despite the simple formulation of this theory, discretization of the plate by means of the finite element comes out to be an important parameter. In many cases, numerical solution can have lack of convergence, which is known as "shear-locking". Shear locking can be avoided by increasing the mesh size, i.e. using finer mesh, but if the thickness/span ratio is "too small", convergence may not be achieved even if the finer mesh is used for the low order displacement shape functions.

In order to avoid shear locking problem, the different methods and techniques, such as reduced and selective reduced integration, the substitute shear strain method, etc., are used by several researchers (Hinton and Huang, 1986; Zienkiewich et al., 1971; Bergan and Wang, 1984; Ozkul and Ture, 2004; Hughes et al., 1977). The same problem can also be prevented by using higher order displacement shape function (Özdemir et al., 2007). Wanji and Cheung (Wanji and Cheung, 2000) proposed a new

* *Corresponding author*. Tel.: +90-462-3774018 ; E-mail address: yozdemir@ktu.edu.tr (Y. I. Özdemir)
ISSN: 2149-8024 / DOI: https://doi.org/10.20528/cjsmec.2018.02.004

quadrilateral thin/thick plate element based on the Mindlin-Reissner theory. Soh et al. (2001) improved a new element ARS-Q12 which is a simple quadrilateral 12 DOF plate bending element based on Reissner-Mindlin theory for analysis of thick and thin plates. Brezzi and Marini (2003) developed a locking free nonconforming element for the Reissner-Mindlin plate using discontinuous Galarkin techniques. Belounar and Guenfound (2005) improved a new rectangular finite element based on the strain approach and the Reissner-Mindlin theory is presented for the analysis of plates in bending either thick or thin. Vibration analysis made by Raju and Hinton (1980), they presented natural frequencies and modes of rhombic Mindlin plates. Si et al. (2005) studied vibration analysis of rectangular plates with one or more guided edges via bicubic B-spline method, Cen et al. (2006) developed a new high performance quadrilateral element for analysis of thick and thin plates. This distinguishing character of the new element is that all formulations are expressed in the quadrilateral area co-ordinate system. Shen et al. (2001) studied free and forced vibration of Reissner-Mindlin plates with free edges resting on elastic foundations. Woo et al. (2003) found accurate natural frequencies and mode shapes of skew plates with and without cutouts by p-version finite element method using integrals of Legendre polynomial for p=1-14. Qian et al. (2003) studied free and forced vibrations of thick rectangular plates using higher-order shear and normal deformable plate theory and meshless Petrov-Galarkin method. Özdemir and Ayvaz (2009) studied shear locking free earthquake analysis of thick and thin plates using Mindlin's theory. GuangPeng et al. (2012) studied free vibration analysis of plates on Winkler elastic foundation by boundary element method. Fallah et al. (2013) analyzed free vibration of moderately thick rectangular FG plates on elastic foundation with various combinations of simply supported and clamed boundary conditions. Governing equations of motion were obtained based on the Mindlin plate theory. Jahromi et al. (2013) analyzed free vibration analysis of Mindlin plates partially resting on Pasternak foundation. The governing equations which consist of a system of partial differential equations are obtained based on the first-order shear deformation theory. Özgan and Daloğlu (2013) studied free vibration analysis of thick plates on elastic foundations using modified Vlasov model with higher order finite elements, also same authors (2015) studied the effects of various parameters such as the aspect ratio, subgrade reaction modulus and thickness/span ratio on the frequency parameters of thick plates resting on Winkler elastic foundations.

The purpose of this paper is to study free vibration analysis of thick plates resting on Winkler foundation using Mindlin's theory with first order finite element, to determine the effects of the thickness/span ratio, the aspect ratio, subgrade reaction modulus and the boundary conditions on the frequency parameters of thick plates subjected to free vibration. A computer program using finite element method is coded in C++ to analyse the plates free, clamped or simply supported along all four edges. In the program, the finite element method is used for spatial integration. Finite element formulation of the equations of the thick plate theory is derived by using first order displacement shape functions. In the analysis, 4-noded finite element is used to construct the stiffness and mass matrices (Özdemir et al., 2007).

2. Mathematical Model

The governing equation for a flexural plate (Fig. 1) subjected to free vibration without damping can be given as;

$$[M]\{\ddot{w}\}+[K]\{w\}=0\ , \tag{1}$$

where [K] and [M] are the stiffness matrix and the mass matrix of the plate, respectively, w and $\ddot{w}$ are the lateral displacement and the second derivative of the lateral displacement of the plate with respect to time, respectively.

The total strain energy of plate-soil-structure system (see Fig. 1) can be written as;

$$\Pi=\Pi_p+\Pi_s+V, \tag{2}$$

where Π_p is the strain energy in the plate,

$$\prod_p=\frac{1}{2}\int_A\left(-\frac{\partial\varphi_x}{\partial x}\quad\frac{\partial\varphi_y}{\partial y}\quad-\frac{\partial\varphi_x}{\partial y}+\frac{\partial\varphi_y}{\partial x}\right)^T E_\kappa\left(-\frac{\partial\varphi_x}{\partial x}\quad\frac{\partial\varphi_y}{\partial y}\quad-\frac{\partial\varphi_x}{\partial y}+\frac{\partial\varphi_y}{\partial x}\right)d_A$$

$$+\frac{k}{2}\int_A\left(-\varphi_x+\frac{\partial w}{\partial x}\quad\varphi_y+\frac{\partial w}{\partial y}\right)^T E_\gamma\left(-\varphi_x+\frac{\partial w}{\partial x}\quad\varphi_y+\frac{\partial w}{\partial y}\right)d_A\ , \tag{3}$$

where Π_s is the strain energy stored in the soil,

$$\prod_s=\frac{1}{2}\int_0^H\int_{-\infty}^{\infty}\int_{-\infty}^{\infty}\sigma_{ij}\varepsilon_{ij}\ , \tag{4}$$

and V is the potential energy of the external loading;

$$V=-\int_A\bar{q}\,w\,d_A\ . \tag{5}$$

In this equation, E_κ and E_γ are the elasticity matrix and these matrices are given below at Eq. (17), $\bar{q}$ shows applied distributed load.

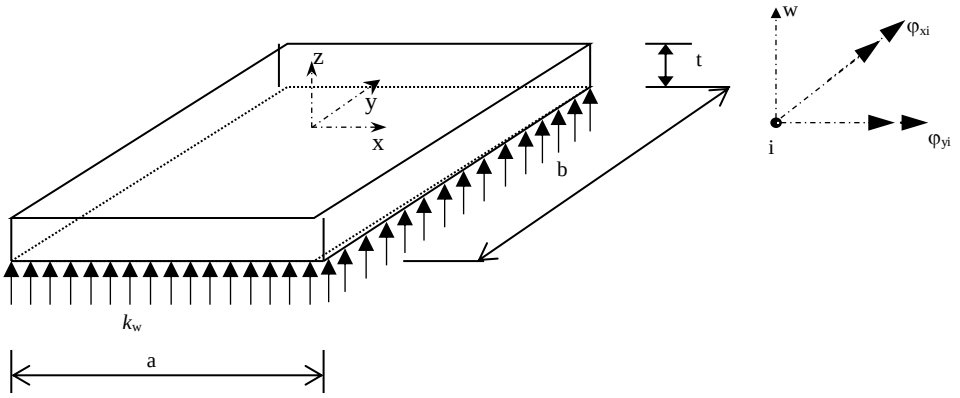

Fig. 1. The sample plate used in this study.

2.1. Evaluation of the stiffness matrix

The total strain energy of the plate-soil system according to Eq. (2) is;

$$U_e = \frac{1}{2}\int_A \left(-\frac{\partial\varphi_x}{\partial x} \quad \frac{\partial\varphi_y}{\partial y} \quad -\frac{\partial\varphi_x}{\partial y}+\frac{\partial\varphi_y}{\partial x}\right)^T E_\kappa \left(-\frac{\partial\varphi_x}{\partial x} \quad \frac{\partial\varphi_y}{\partial y} \quad -\frac{\partial\varphi_x}{\partial y}+\frac{\partial\varphi_y}{\partial x}\right) d_A$$
$$+\frac{k}{2}\int_A \left(-\varphi_x+\frac{\partial w}{\partial x} \quad \varphi_y+\frac{\partial w}{\partial y}\right)^T E_\gamma \left(-\varphi_x+\frac{\partial w}{\partial x} \quad \varphi_y+\frac{\partial w}{\partial y}\right) d_A + \frac{1}{2}\int_A \left(w_{x,y}\right)^T \mathrm{K}\left(w_{x,y}\right) d_A \ . \tag{6}$$

At this equation the first and second part gives the conventional element stiffness matrix of the plate, $[k_p^e]$, differentiation of the third integral with respect to the nodal parameters yields a matrix, $[k_w^e]$, which accounts for the axial strain effect in the soil. Thus the total energy of the plate-soil system can be written as;

$$U_e = \frac{1}{2}\{w_e\}^T \left(\left[k_p^e\right]+\left[k_w^e\right]\right)\{w_e\} d_A \ , \tag{7}$$

where

$$\{w_e\} = \begin{bmatrix} w_1 & \varphi_{x1} & \varphi_{y1} & \dots & w_n & \varphi_{xn} & \varphi_{yn} \end{bmatrix}^T \ . \tag{8}$$

Assuming that in the plate of Fig. 1 u and v are proportional to z and that w is the independent of z (Mindlin, 1951), one can write the plate displacement at an arbitrary x, y, z in terms of the two slopes and a displacement as follows;

$$\{w,\ u,\ v\} = \{w,\ z\varphi_x,\ -z\varphi_y\} = \{w,\ z\frac{\partial\varphi_i}{\partial x}, -z\frac{\partial\varphi_i}{\partial y}\} \ , \tag{9}$$

where w_0 is average displacement of the plate and, φ_x and φ_y are the bending slopes in the x and y directions, respectively.

The nodal displacements for 4-noded quadrilateral serendipity element (MT4) (Fig. 2) can be written as follows;

$$w = \sum h_{i1} w_i \ , \quad u = z\varphi_x = z\sum_1^4 h_{i2}\varphi_{xi} \ ,$$
$$v = -z\varphi_y = -z\sum_1^4 h_{i3}\varphi_{yi} \ , \quad (i=1, 2, 3, 4) \ . \tag{10}$$

Nodal actions corresponding to the displacements in Eq. (10) are;

$$\mathrm{pi} = \{\mathrm{p_{i1}}, \mathrm{p_{i2}}, \mathrm{p_{i3}}\} = \{\mathrm{p_{zi}}, \mathrm{M_{xi}}, \mathrm{M_{yi}}\} \quad (\mathrm{i}=1, 2, 3, 4) \ . \tag{11}$$

The symbols p_{zi} denotes a force in the z direction, but M_{xi} and M_{yi} are moments in the x and y directions. Note that these fictitious moments at the nodes are not the same as the distributed moments in the vector M of generalized stresses (Weaver and Johnston, 1984).

The displacement function chosen for this element is;

$$w = \mathrm{c_1} + \mathrm{c_2} r + \mathrm{c_3} s + \mathrm{c_4} rs \ , \tag{12}$$

which is a complete linear of four terms. From this assumption, it is possible to derive the displacement shape function to be;

$$\mathrm{h_i} = [\mathrm{h_1}, \mathrm{h_2}, \mathrm{h_3}, \mathrm{h_4}] \ , \tag{13}$$

where

$$\mathrm{h_1} = (0.25) \times (1+r) \times (1+s) \ ,$$
$$\mathrm{h_2} = (0.25) \times (1-r) \times (1+s) \ ,$$
$$\mathrm{h_3} = (0.25) \times (1-r) \times (1-s) \ ,$$
$$\mathrm{h_4} = (0.25) \times (1+r) \times (1-s) \ . \tag{14}$$

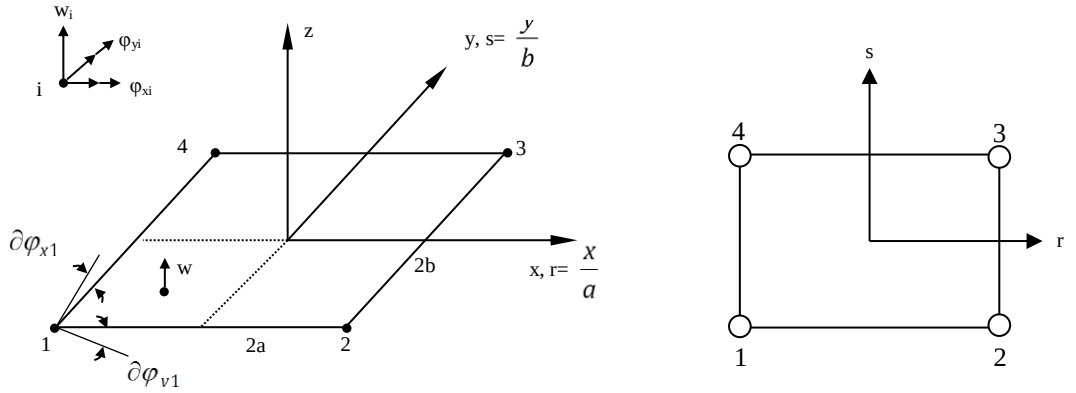

Fig. 2. 4-noded (first order) quadrilateral finite element used in this study (Weaver and Johnston, 1984).

The 3x3 Jacobian matrix required in this formulation is;

$$J=\begin{bmatrix}0 & x_r & y_r\\ 0 & x_s & y_s\\ 1 & 0 & 0\end{bmatrix}, \tag{15}$$

where

$$\begin{aligned} x_r &= \sum_{i=1}^{4}\left(h_{i,r}x_i\right)\ldots\ldots\ldots\ldots\ldots\ldots y_r = \sum_{i=1}^{4}\left(h_{i,r}y_i\right)\\ x_s &= \sum_{i=1}^{4}\left(h_{i,s}x_i\right)\ldots\ldots\ldots\ldots\ldots\ldots y_s = \sum_{i=1}^{4}\left(h_{i,s}y_i\right)\end{aligned}. \tag{16}$$

The inverse of J becomes

$$J^{-1}=\begin{bmatrix}0 & r_x & s_x\\ 0 & r_y & s_y\\ 1 & 0 & 0\end{bmatrix}. \tag{17}$$

We need certain derivatives with respect to local coordinates, which are placed into a 3x3 matrix;

$$\begin{bmatrix}w_r & u_r & v_r\\ w_s & u_s & v_s\\ w_z & u_z & v_z\end{bmatrix}=\sum_{i=1}^{4}\begin{bmatrix}f_{i,r}w_i & zf_{i,r}\varphi_{xi} & -zf_{i,r}\varphi_{yi}\\ f_{i,s}w_i & zf_{i,s}\varphi_{xi} & -zf_{i,s}\varphi_{yi}\\ 0 & f_i\varphi_{xi} & -f_i\varphi_{yi}\end{bmatrix}. \tag{18}$$

Transformation of these derivatives to global coordinates is accomplished using the inverse of the Jacobian matrix, as follows;

$$\begin{bmatrix}w_x & u_x & v_x\\ w_y & u_y & v_y\\ w_z & u_z & v_z\end{bmatrix}=J^{-1}\begin{bmatrix}w_r & u_r & v_r\\ w_s & u_s & v_s\\ w_z & u_z & v_z\end{bmatrix}. \tag{19}$$

The five types of nonzero strains to be considered for this element are;

$$\varepsilon=\begin{bmatrix}\varepsilon_x\\ \varepsilon_y\\ \gamma_{xy}\\ \gamma_{xz}\\ \gamma_{yz}\end{bmatrix}=\begin{bmatrix}u_x\\ v_y\\ u_y+v_x\\ u_z+w_x\\ v_z+w_y\end{bmatrix}. \tag{20}$$

As a preliminary matter before formulating element stiffness matrix, matrix B partitioned and *z* factored from the upper part, as follows (Cook et al., 1989);

$$B=\begin{bmatrix}B_k\\ B_\gamma\end{bmatrix}=\begin{bmatrix}z\overline{B}_k\\ B_\gamma\end{bmatrix}, \tag{21}$$

where B_k has three rows and B_γ has two rows, then the stiffness matrix for this element is written as;

$$\begin{aligned} K &= \int_V B^T E B dV = \int_V \begin{bmatrix}z\overline{B}_k^T & B_\gamma^T\end{bmatrix}\begin{bmatrix}E_k & 0\\ 0 & E_\gamma\end{bmatrix}\begin{bmatrix}z\overline{B}_k^T\\ B_\gamma^T\end{bmatrix}dV\\ K &= \int_V \left(z^2\overline{B}_k^T E_k \overline{B}_k\right)+\left(\overline{B}_\gamma^T E_\gamma \overline{B}_\gamma\right)dV\end{aligned}. \tag{22}$$

Integration through the thickness yields;

$$K=\int_A\left(\overline{B}_k^T\overline{E}_k\overline{B}_k+\overline{B}_\gamma^T\overline{E}_\gamma\overline{B}_\gamma\right)dA. \tag{23}$$

Thus,

$$K=\int_A \overline{B}^T\overline{E}\overline{B}dA=\int_{-1}^{1}\int_{-1}^{1}\overline{B}^T\overline{E}\overline{B}|J|drds, \tag{24}$$

which must be evaluated numerically (Hughes et al., 1977).

In this equation, $[E_k]$ is of size 3x3 and $[E_\gamma]$ is of size 2x2. $[E_k]$, and $[E_\gamma]$ can be written as follows (Bathe, 1996; Weaver and Johston, 1984):

$$[E_k]=\frac{t^3}{12}\begin{bmatrix} \frac{E}{(1-\nu^2)} & \frac{\nu E}{(1-\nu^2)} & 0 \\ \frac{\nu E}{(1-\nu^2)} & \frac{E}{(1-\nu^2)} & 0 \\ 0 & 0 & \frac{E}{2(1-\nu)} \end{bmatrix},$$

$$[E_\gamma]=kt\begin{bmatrix} \frac{E}{2.4(1+\nu)} & 0 \\ 0 & \frac{E}{2.4(1+\nu)} \end{bmatrix}, \quad (25)$$

where E, υ, and t are modulus of the elasticity, Poisson's ratio, and the thickness of the plate, respectively, k is a constant to account for the actual non-uniformity of the shearing stresses. By assembling the element stiffness matrices obtained, the system stiffness matrix is obtained.

2.2. Evaluation of the mass matrix

The formula for the consistent mass matrix of the plate may be written as

$$M=\int_\Omega H_i^T \mu H_i d\Omega \ . \quad (26)$$

In this equation, μ is the mass density matrix of the form (Tedesco et al., 1999).

$$\mu=\begin{bmatrix} m_1 & 0 & 0 \\ 0 & m_2 & 0 \\ 0 & 0 & m_3 \end{bmatrix}, \quad (27)$$

where $m_1=\rho_p t$, $m_2=m_3=\frac{1}{12}\left(\rho_p t^3\right)$, and ρ_p is the mass densities of the plate. And H_i can be written as follows,

$$H_i=\begin{bmatrix} dh_i/dx & dh_i/dy & h_i \end{bmatrix} \qquad i=1\ldots 17. \quad (28)$$

It should be noted that the rotation inertia terms are not taken into account. By assembling the element mass matrices obtained, the system mass matrix is obtained.

2.3. Evaluation of the frequency of plate

The formulation of lateral displacement, w, can be given as motion is sinusoidal;

$$w=W\sin\omega t. \quad (29)$$

Here ω is the circular frequency. Substitution of Eq. (29) and its second derivation into Eq. (1) gives expression as;

$$[\mathrm{K}-\omega^2\mathrm{M}]\{W\}=0. \quad (30)$$

Eq. (30) is obtained to calculate the circular frequency, ω, of the plate. Then natural frequency can be calculated with the formulation below;

$$F=\omega/2\pi. \quad (31)$$

3. Numerical Examples

3.1. Data for numerical examples

In the light of the results given in references (Özdemir et al., 2007; Özdemir, 2012), the aspect ratios, b/a, of the plate are taken to be 1, 1.5, and 2.0. The thickness/span ratios, t/a, are taken as 0.05, 0.1, and 0.2 for each aspect ratio. The shorter span length of the plate is kept constant to be 10 m. The mass density, Poisson's ratio, and the modulus of elasticity of the plate are taken to be 2.5 kN s^2/m^2, 0.2, and 2.7x10^7 kN/m^2. Shear factor k is taken to be 5/6. The subgrade reaction modulus of the Winkler-type foundation is taken to be 500 and 5000 kN/m^3.

For the sake of accuracy in the results, rather than starting with a set of a finite element mesh size, the mesh size required to obtain the desired accuracy were determined before presenting any results. This analysis was performed separately for the mesh size. It was concluded that the results have acceptable error when equally spaced 20x20 mesh size for 4-noded elements are used for a 10 m x 10 m plate. Length of the elements in the x and y directions are kept constant for different aspect ratios as in the case of square plate.

In order to illustrate that the mesh density used in this paper is enough to obtain correct results, the first six frequency parameters of the thick plate with b/a=1 and t/a=0.05 is presented in Table 1 by comparing with the result obtained SAP2000 program and the results Özgan and Daloğlu (2015). In this study Özgan and Daloğlu used 4-noded and 8-noded quadrilateral finite element with 10x10 and 5x5 mesh size. It should be noted that the results presented for MT4 element are obtained by using equally spaced 20x20 mesh size.

3.2. Results

The first six frequency parameters of thick plate resting on Winkler foundation with free edges are compared with the same thick plate modeled by Özgan and Daloğlu (2010) and SAP program and it is presented in Table1. The subgrade reaction modulus of the Winkler-type foundation for this example is taken to be 5000 kN/m^3. This thick plate is modeled with MT4 element 20x20 mesh size for b/a=1.0, t/a =0.05 ratios.

As seen from Table 1, the values of the frequency parameters of these analyses are so close. Then writers enlarged parameters of aspect ratio, b/a, thickness/span ratio, t/a, for help the researchers.

The first six frequency parameters of thick plates resting on Winkler foundation considered for different aspect ratio, b/a, thickness/smaller span ratio, t/a, are presented in Table 2 for the with free edges, in Table 3 for thick clamped plates. In order to see the effects of the changes in these parameters better on the first six frequency parameters, they are also presented in Figs. 3-4 for the thick free plates, in Figs. 5-6 for the thick clamped plates.

As seen from Table 2, and Figs. 3, and 4, the values of the first three frequency parameters for a constant value of t/a increase as the aspect ratio, b/a, increases up to the 3rd frequency parameters, but after the 3rd frequency parameter, the values of the frequency parameters for a constant value of t/a decrease as the aspect ratio, b/a, increases.

Table 1. The first five natural frequency parameters of plates for b/a=1 and t/a=0.05.

$\lambda_i=\omega^2$	Özgan and Daloğlu (2015)	This Study	SAP2000
	PBQ8(FI)	MT4 (400 element)	
1	3990.42	4061.49	4000.00
2	3990.42	4061.49	4000.00
3	4000.40	4082.22	4000.00
4	8676.00	8762.37	8619.60
5	13957.64	17776.58	13292.31
6	17252.34	20960.35	16380.24

Table 2. Effects of aspect ratio and thickness/span ratio on the first six frequency parameters of the thick free plates resting on elastic foundation.

a) Subgrade reaction modulus k=500

k	b/a	t/a	$\lambda=\omega^2$					
			λ_1	λ_2	λ_3	λ_4	λ_5	λ_6
500	1.0	0.05	430	430	438	5140	14176	17357
		0.10	199	199	212	17645	41441	53335
		0.20	94	94	106	58997	130338	168555
	1.5	0.05	431	434	440	2515	3440	11923
		0.10	201	206	214	8026	9643	40293
		0.20	94	100	107	27419	32615	128500
	2.0	0.05	432	436	440	1389	1587	6159
		0.10	202	209	215	3235	4565	20820
		0.20	94	103	107	10912	15545	69111

b) Subgrade reaction modulus k=5000

k	b/a	t/a	$\lambda=\omega^2$					
			λ_1	λ_2	λ_3	λ_4	λ_5	λ_6
5000	1.0	0.05	4061	4061	4082	8762	17777	20960
		0.10	2028	2028	2045	19466	43226	55118
		0.20	981	981	1024	59866	131150	169372
	1.5	0.05	4064	4072	4084	6143	7064	15539
		0.10	2029	2039	2048	9852	11457	42102
		0.20	981	1004	1024	28299	33479	129354
	2.0	0.05	4065	4077	4086	5023	5217	9783
		0.10	2029	2043	2048	5059	6392	22637
		0.20	981	1013	1024	11798	16428	69980

Table 3. Effects of aspect ratio and thickness/span ratio on the first six frequency parameters of the thick clamped plates resting on elastic foundation.

a) Subgrade reaction modulus k=500

k	b/a	t/a	$\lambda = \omega^2$					
			λ_1	λ_2	λ_3	λ_4	λ_5	λ_6
500	1.0	0.05	36939	149205	149205	301078	472059	477466
		0.10	108466	402992	402992	787956	1126271	1156881
		0.20	283837	885712	885712	1603877	2126830	2185266
	1.5	0.05	21497	48713	123073	125433	171534	274339
		0.10	63733	143687	338076	343965	466814	733072
		0.20	175581	371188	752882	801534	1022285	1535569
	2.0	0.05	18205	28853	55872	111646	119141	140610
		0.10	53571	86512	165072	317108	319958	382361
		0.20	148609	234915	425641	713638	760071	849653

b) Subgrade reaction modulus k=5000

k	b/a	t/a	$\lambda = \omega^2$					
			λ_1	λ_2	λ_3	λ_4	λ_5	λ_6
5000	1.0	0.05	40570	152816	152816	304670	475641	481049
		0.10	110264	404763	404763	789707	1138013	1158626
		0.20	284721	886575	886575	1604729	2127672	2186119
	1.5	0.05	25132	52339	126684	129048	175139	277932
		0.10	65537	145475	339851	345734	468578	734821
		0.20	176470	372061	753747	802393	1023142	1536418
	2.0	0.05	21842	32485	59495	115257	122757	144221
		0.10	55377	88309	166856	318876	321736	384131
		0.20	149500	235795	426509	714505	760927	850513

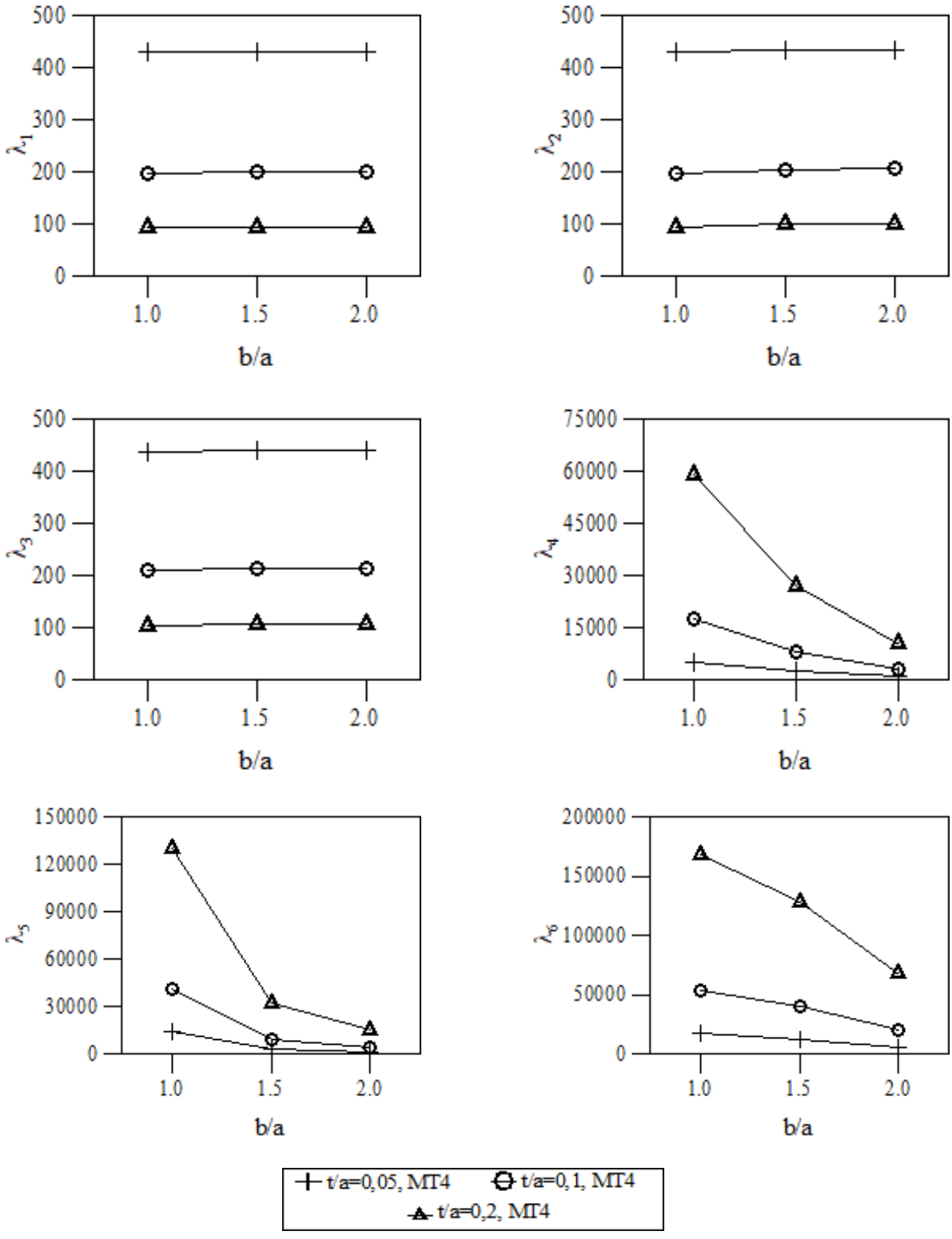

Fig. 3. Effects of aspect ratio and thickness/span ratio on the first six frequency parameters of the thick free plates with subgrade reaction modulus k=500.

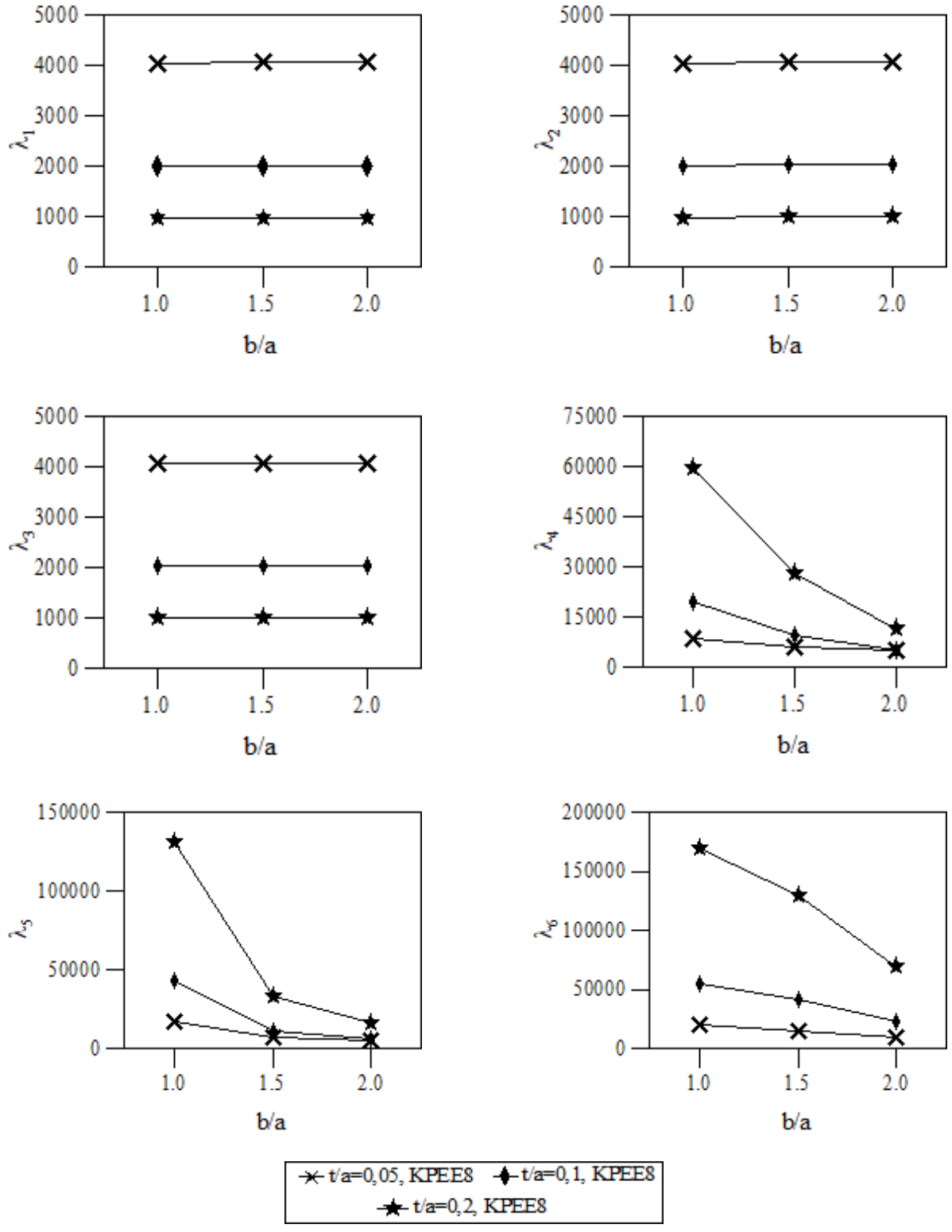

Fig. 4. Effects of aspect ratio and thickness/span ratio on the first six frequency parameters of the thick free plates with subgrade reaction modulus k=5000.

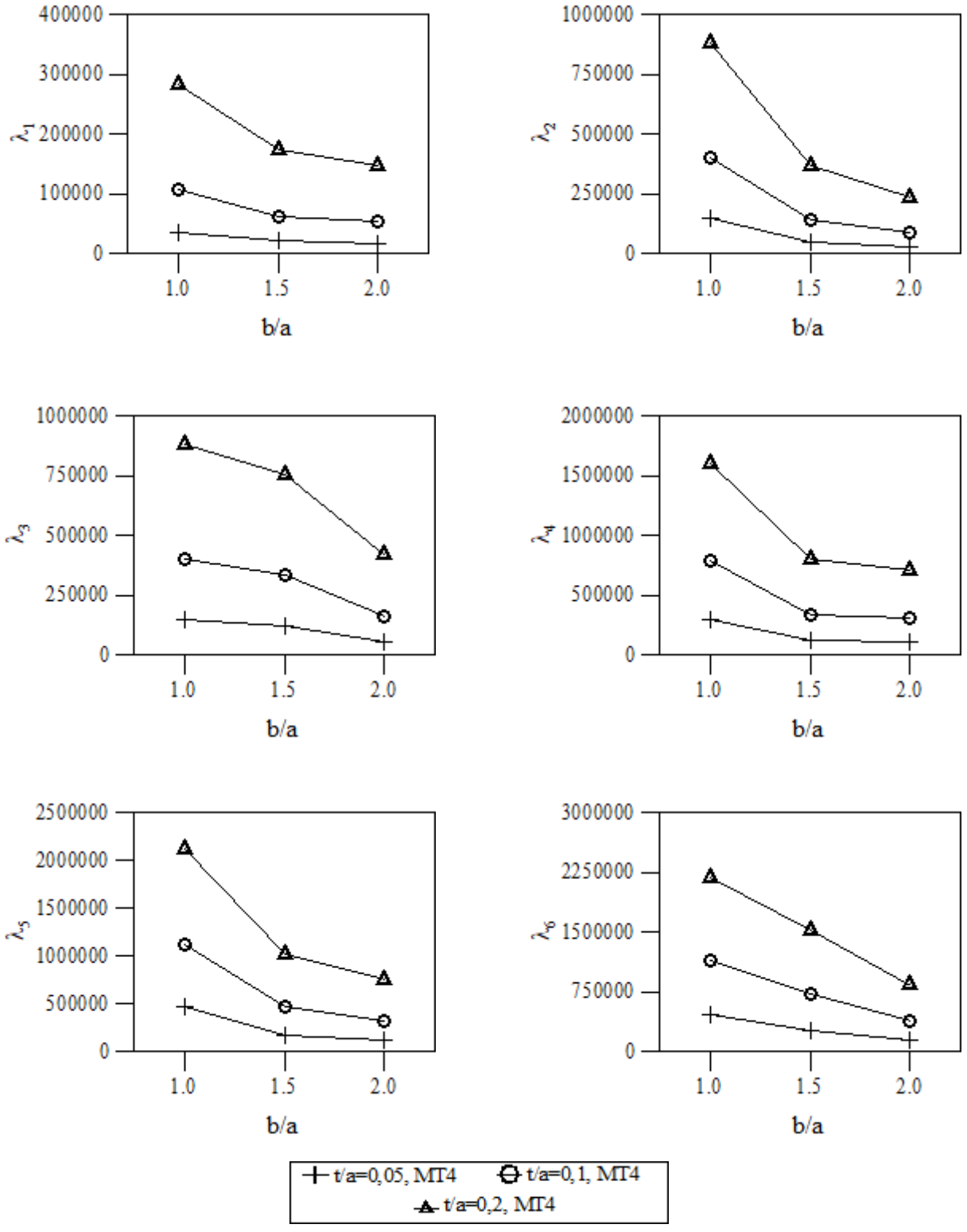

Fig. 5. Effects of aspect ratio and thickness/span ratio on the first six frequency parameters of the thick clamped plates with subgrade reaction modulus k=500.

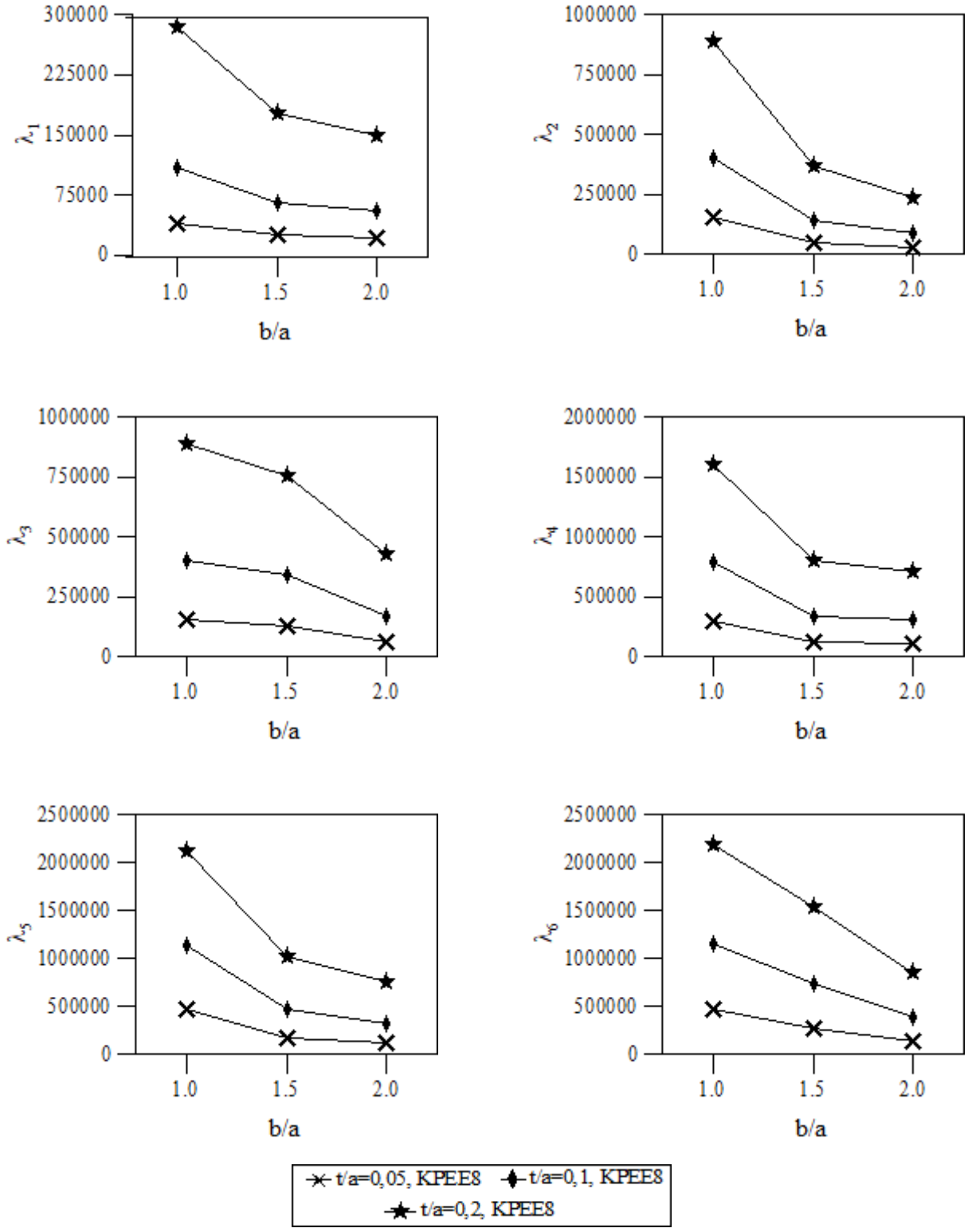

Fig. 6. Effects of aspect ratio and thickness/span ratio on the first six frequency parameters of the thick clamped plates with subgrade reaction modulus k=5000.

As also seen from Table 2 and, Figs. 3 and 4, the values of the first three frequency parameters for a constant value of b/a decrease as the thickness/span ratio, t/a, increases up to the 3rd frequency parameters, but after the 3rd frequency parameters, the values of the frequency parameters for a constant value of b/a increase as the thickness/span ratio, t/a, increases.

The increase in the frequency parameters with increasing value of b/a for a constant t/a ratio gets less for larger values of b/a up to the 3rd frequency parameters. After the 3rd frequency parameters, the decrease in the frequency parameters with increasing value of b/a for a constant t/a ratio gets also less for larger values of b/a.

The changes in the frequency parameters with increasing value of b/a for a constant t/a ratio is larger for the smaller values of the b/a ratios. Also, the changes in the frequency parameters with increasing value of b/a for a constant t/a ratio is less than in the frequency parameters with increasing t/a ratios for a constant value of b/a.

These observations indicate that the effects of the change in the t/a ratio on the frequency parameter of the plate are generally larger than those of the change in the b/a ratios considered in this study.

As also seen from Table 2 and, Figs. 3 and 4, the curves for a constant value of b/a ratio are fairly getting closer to each other as the value of t/a increases up to the 3rd frequency parameters. This shows that the curves of the frequency parameters will almost coincide with each other when the value of the ratio of t/a increases more. After the 3rd frequency parameters, the curves for a constant value of t/a ratio are fairly getting closer to each other as the value of b/a increases. This also shows that the curves of the frequency parameters will almost coincide with each other when the value of the ratio of b/a increases more.

In other words, up to the 3rd frequency parameters, the increase in the t/a ratio will not affect the frequency parameters after a determined value of t/a. After the 3rd frequency parameters, the increase in the b/a ratio will not affect the frequency parameters after a determined value of b/a.

As seen from Table 3 and, Figs. 5 and 6, the values of the frequency parameters for a constant value of t/a decrease as the aspect ratio, b/a, increases. This behavior is understandable in that a thick plate with a larger aspect ratio becomes more flexible and has smaller frequency parameters. The decreases in the frequency parameters with increasing value of b/a ratio gets less for a constant value of t/a.

As seen from Table 3 and, Figs. 5 and 6, the values of the frequency parameters for a constant value of b/a increase as the thickness/span ratio, t/a, increases. This behavior is also understandable in that a thick plate with a larger thickness/span ratio becomes more rigid and has larger frequency parameters. The increases in the frequency parameters with increasing value of t/a ratio gets larger for a constant value of b/a.

It should be noted that the increase in the frequency parameters with increasing t/a ratios for a constant value of b/a ratio gets larger for larger values of the frequency parameters.

These observations indicate that the effects of the change in the t/a ratio on the frequency parameter of the thick plates clamped along all four edges are always larger than those of the change in the aspect ratio.

As also seen from Figs. 3, 4, 5 and 6, the curves for a constant value of the aspect ratio, b/a are fairly getting closer to each other as the value of t/a decreases. This shows that the curves of the frequency parameters will almost coincide with each other when the value of the thickness/span ratio, t/a, decreases more. In other words, the decrease in the thickness/span ratio will not affect the frequency parameters after a determined value of b/a.

In this study, the mode shapes of the thick plates are also obtained for all parameters considered. Since presentation of all of these mode shapes would take up excessive space, only the mode shapes corresponding to the six lowest frequency parameters of the thick plate free, clamped along all four edges for $b/a = 1$, and 2 and $t/a = 0.05$ are presented. These mode shapes are given in Figs. 7, 8 and 9, respectively. In order to make the visibility better, the mode shapes are plotted with exaggerated amplitudes.

As seen from these figures, the number of half wave increases as the mode number increases. It should be noted that appearances of the mode shapes not given here for the thick plates clamped along all four edges are similar to those of the mode shapes presented here.

4. Conclusions

The purpose of this paper was to study parametric free vibration analysis of thick plates using first order finite elements with Mindlin's theory and to determine the effects of the thickness/span ratio, the aspect ratio and the boundary conditions on the linear responses of thick plates subjected to vibration. As a result, free vibration analyze of the thick plates were done by using first order serendipity element, and the coded program on the purpose is effectively used. In addition, the following conclusions can also be drawn from the results obtained in this study.

The frequency parameters increases with increasing b/a ratio for a constant value of t/a up to the 3rd frequency parameters, but after that the frequency parameters decreases with increasing b/a ratio for a constant value of t/a.

The frequency parameters decreases with increasing t/a ratio for a constant value of b/a up to the 3rd frequency parameters, but after that the frequency parameters increases with increasing t/a ratio for a constant value of b/a.

The effects of the change in the t/a ratio on the frequency parameter of the thick plate are generally larger than those of the change in the b/a ratios considered in this study.

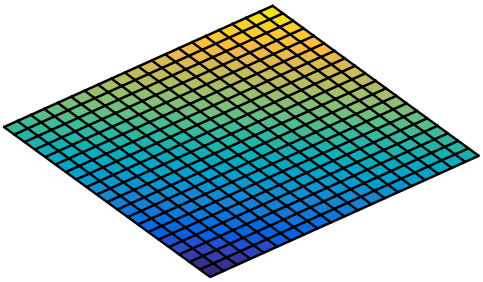

The first mode shape
(λ_1=4061)

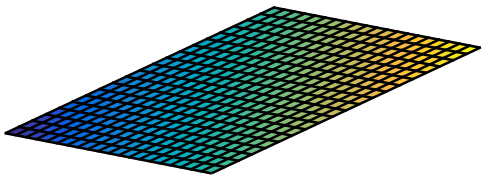

The second mode shape
(λ_2=4061)

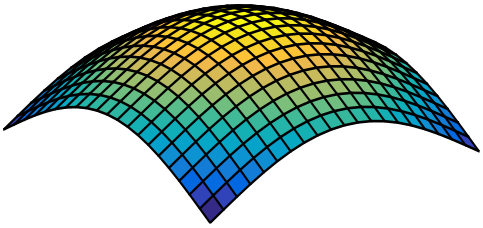

The third mode shape
(λ_3=4082)

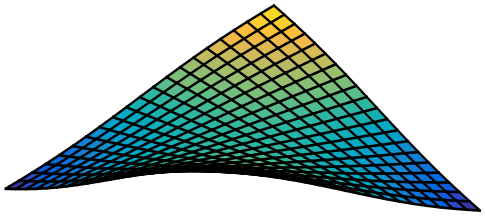

The fourth mode shape
(λ_4=8762)

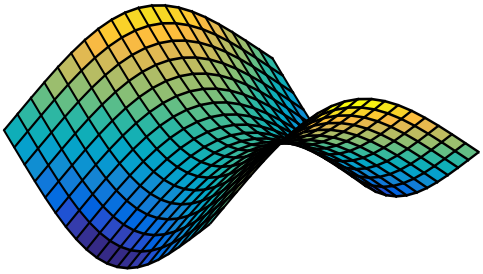

The fifth mode shape
(λ_5=17777)

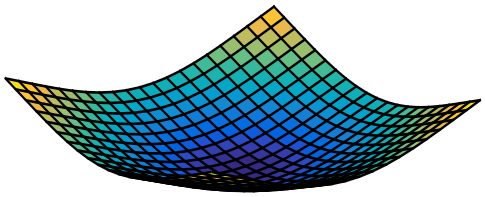

The sixth mode shape
(λ_6=20960)

Fig. 7. The first six mode shapes of the thick free plates for b/a=1.0 and t/a=0.05 with subgrade reaction modulus k=5000.

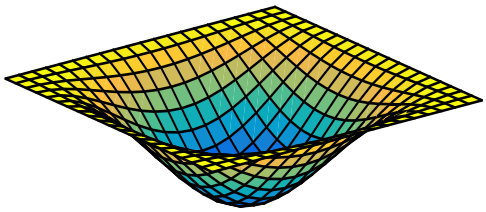

The first mode shape
(λ_1=40570)

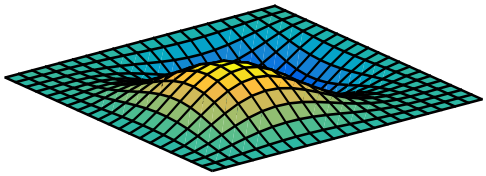

The second mode shape
(λ_2=152816)

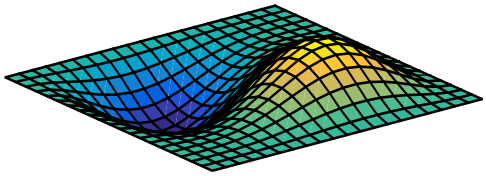

The third mode shape
(λ_3=152816)

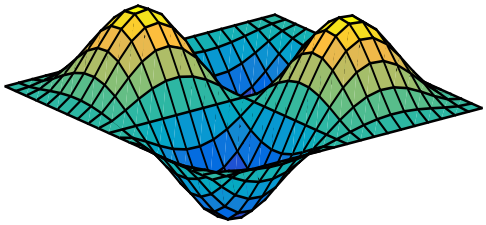

The fourth mode shape
(λ_4=304670)

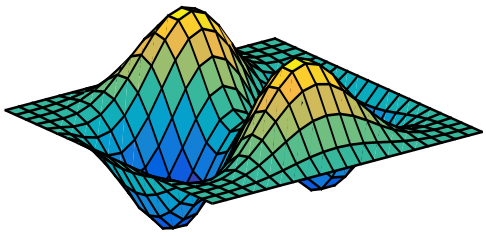

The fifth mode shape
(λ_5=475641)

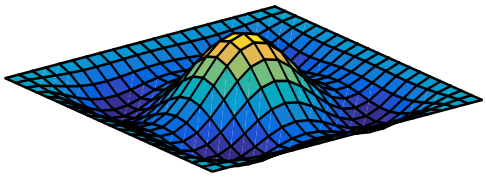

The sixth mode shape
(λ_6=481049)

Fig. 8. The first six mode shapes of the thick clamped plates for b/a=1.0 and t/a=0.05 with subgrade reaction modulus k=5000.

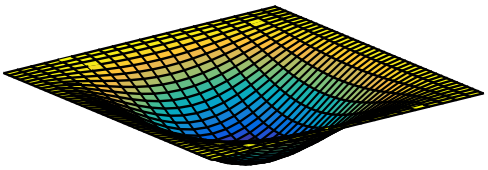

The first mode shape
(λ_1=21842)

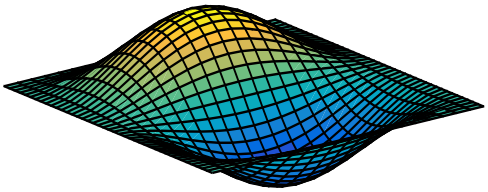

The second mode shape
(λ_2=32485)

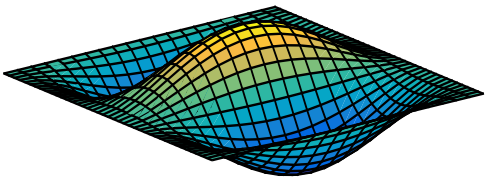

The third mode shape
(λ_3=59495)

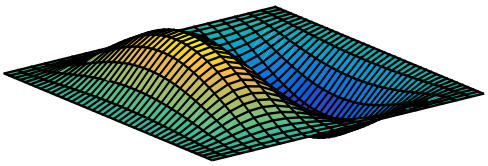

The fourth mode shape
(λ_4=115257)

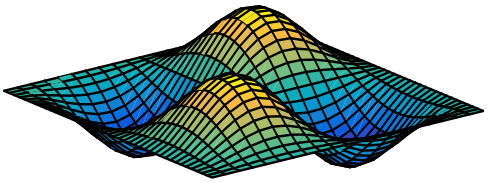

The fifth mode shape
(λ_5=122757)

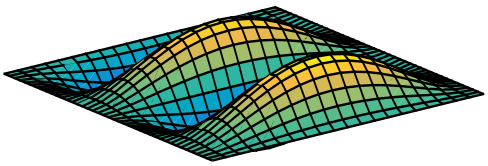

The sixth mode shape
(λ_6=144221)

Fig. 9. The first six mode shapes of the thick clamped plates for b/a=2.0 and t/a=0.05 with subgrade reaction modulus k=5000.

REFERENCES

Ayvaz Y, Durmuş A (1995). Earthquake analysis of simply supported reinforced concrete slabs. *Journal of Sound & Vibration,* 187(3), 531-539.

Bathe KJ (1996). Finite Element Procedures. Prentice Hall, Upper Saddle River, New Jersey.

Belounar L, Guenfound M (2005). A new rectangular finite element based on the strain approach for plate bending. *Thin-Walled Structures,* 43, 47-63.

Bergan PG, Wang X (1984). Quadrilateral plate bending elements with shear deformations. *Computers & Structures,* 19(1-2) 25-34.

Brezzi F, Marini LD (2003). A nonconforming element for the Reissner-Mindlin plate. *Computers & Structures,* 81, 515-522.

Caldersmith GW (1984). Vibrations of orthotropic rectangular plates. *ACUSTICA,* 56, 144-152.

Cen S, Long YQ, Yao ZH, Chiew SP (2006). Application of the quadrilateral area co-ordinate method: Anew element for Mindlin-Reissner plate. *International Journal of Numerical Methods in Engineering,* 66, 1-45.

Cook RD, Malkus DS, Michael EP (1989). Concepts and Applications of Finite Element Analysis. John Wiley & Sons, Inc., Canada.

Fallah A, Aghdam MM, Kargarnovin MH (2013). Free vibration analysis of moderately thick functionally graded plates on elastic foundation using the extended Kantorovich method. *Archive of Applied Mechanics,* 83(2), 177-191.

Grice RM, Pinnington RJ (2002). Analysis of the flexural vibration of a thin-plate box using a combination of finite element analysis and analytical impedances. *Journal of Sound & Vibration,* 249(3), 499-527.

Gunagpeng Z, Tianxia Z, Yaohui S (2012). Free vibration analysis of plates on Winkler elastic foundation by boundary element method. *Optical and Electronics Materials Applications II*, 529, 246-251.

Hinton E, Huang HC (1986). A family of quadrilateral Mindlin plate element with substitute shear strain fields. *Computers & Structures,* 23(3), 409-431.

Hughes TJR, Taylor RL, Kalcjai W (1977). Simple and efficient element for plate bending. *International Journal of Numerical Methods in Engineering,* 11, 1529-1543.

Jahromi HN, Aghdam MM, Fallah A (2013). Free vibration analysis of Mindlin plates partially resting on Pasternak foundation. *International Journal of Mechanics and Sciences*, 75, 1-7.

Leissa AW (1973). The free vibration of rectangular plates. *Journal of Sound & Vibration,* 31(3), 257-294.

Leissa AW (1977a). Recent research in plate vibrations, 1973–1976: classical theory, *The Shock and Vibration Digest,* 9(10), 13–24.

Leissa AW (1977b). Recent research in plate vibrations, 1973–1976: complicating effects. *The Shock and Vibration Digest,* 9(11), 21–35.

Leissa AW (1981a). Plate vibration research, 1976–1980: classical theory. *The Shock and Vibration Digest,* 13(9), 11–22.

Leissa AW (1981b). Plate vibration research, 1976–1980: complicating effects. *The Shock and Vibration Digest,* 13(10) 19–36.

Leissa AW (1987a). Plate vibration research, 1981–1985—part I: classical theory. *The Shock and Vibration Digest,* 19(2), 11–18.

Leissa AW (1987b). Plate vibration research, 1981–1985—part II: complicating effects, *The Shock and Vibration Digest,* 19(3), 10–24.

Lok TS, Cheng QH (2001). Free and forced vibration of simply supported, orthotropic sandwich panel. *Computers & Structures,* 79(3), 301-312.

Mindlin RD (1951). Influence of rotatory inertia and shear on flexural motions of isotropic, elastic plates. *Journal of Applied Mechanics (ASME),* 18(1), 31-38.

Özdemir YI (2012). Development of a higher order finite element on a Winkler foundation. *Finite Element Analysis and Design,* 48, 1400-1408.

Özdemir YI, Ayvaz Y (2009). Shear locking-free earthquake analysis of thick and thin plates using Mindlin's theory. *Structural Engineering & Mechanics,* 33(3), 373-385.

Özdemir YI, Bekiroğlu S, Ayvaz Y (2007). Shear locking-free analysis of thick plates using Mindlin's theory. *Structural Engineering & Mechanics,* 27(3), 311-331.

Özgan K, Daloğlu AT (2012). Free vibration analysis of thick plates on elastic foundations using modified Vlasov model with higher order finite elements. *International Journal of Engineering & Materials Sciences,* 19, 279-291.

Özgan K, Daloğlu AT (2015). Free vibration analysis of thick plates resting on Winkler elastic foundation. *Challenge Journal of Structural Mechanics,* 1(2), 78-83.

Özkul TA, Ture U (2004). The transition from thin plates to moderately thick plates by using finite element analysis and the shear locking problem. *Thin-Walled Structures*, 42, 1405-1430.

Providakis CP, Beskos DE (1989a). Free and forced vibrations of plates by boundary elements. *Computer Methods in Applied Mechanical Engineering,* 74, 231-250.

Providakis CP, Beskos DE (1989b). Free and forced vibrations of plates by boundary and interior elements. *International Journal of Numerical Methods in Engineering,* 28, 1977-1994.

Qian LF, Batra RC, Chen LM (2003). Free and forced vibration of thick rectangular plates using higher-order shear and normal deformable plate theory and meshless Petrov-Galerkin (MLPG) method. *Computer Modeling Engineering & Sciences,* 4(5), 519-534.

Raju KK, Hinton E (1980). Natural frequencies and modes of rhombic Mindlin plates. *Earthquake Engineering Structural Dynamics,* 8, 55-62.

Reissner E (1945). The effect of transverse shear deformation on the bending of elastic plates. *Journal of Applied Mechanics (ASME),* 12, A69-A77.

Reissner E (1947). On bending of elastic plates. *Quarterly Applied Mathematics,* 5(1), 55-68.

Reissner E (1950). On a variational theorem in elasticity. *Journal of Mathematics and Physics,* 29, 90-95.

Sakata T, Hosokawa K (1988). Vibrations of clamped orthotropic rectangular plates. *Journal of Sound & Vibration,* 125(3), 429-439.

Shen HS, Yang J, Zhang L (2001). Free and forced vibration of Reissner-Mindlin plates with free edges resting on elastic foundation. *Journal of Sound & Vibration,* 244(2), 299-320.

Si WJ, Lam KY, Gang SW (2005). Vibration analysis of rectangular plates with one or more guided edges via bicubic B-spline method. *Shock & Vibration,* 12(5), 363-376.

Soh AK, Cen S, Long Y, Long Z (2001). A new twelve DOF quadrilateral element for analysis of thick and thin plates. *European Journal of Mechanics: A/Solids,* 20, 299-326.

Tedesco JW, McDougal WG, Ross CA (1999). Structural Dynamics. Addison Wesley Longman Inc., California.

Ugural AC (1981). Stresses in Plates and Shells. McGraw-Hill., New York.

Wanji C, Cheung YK (2000). Refined quadrilateral element based on Mindlin/Reissner plate theory. *International Journal of Numerical Methods in Engineering,* 47, 605-627.

Warburton GB (1954). The vibration of rectangular plates. *Proceeding of the Institute of Mechanical Engineers* 168, 371-384.

Weaver W, Johnston PR (1984). Finite Elements for Structural Analysis. Prentice Hall, Inc., Englewood Cliffs, New Jersey.

Woo KS, Hong CH, Basu PK, Seo CG (2003). Free vibration of skew Mindlin plates by p-version of F.E.M. *Journal of Sound & Vibration,* 268, 637-656.

Zienkiewich OC, Taylor RL, Too JM (1971). Reduced integration technique in general analysis of plates and shells. *International Journal of Numerical Methods in Engineering,* 3, 275-290.